Inorg. Chem. **2006**, *45*, 10002–10012

Forum

Of Folding and Function: Understanding Active-Site Context through Metalloenzyme Design

Kinesha L. Harris, Sunghyuk Lim, and Sonya J. Franklin*

Department of Chemistry, University of Iowa, Iowa City, Iowa 52242

Received May 19, 2006

In the emerging field of biomolecular design, the introduction of metal-binding sites into loop or turn regions of known protein scaffolds has been utilized to create unique metalloprotein and metallopeptide systems for study. This Forum Article highlights examples of the modular-turn-substitution approach to design and the range of structural and mechanistic questions to which this tool can be applied. Examples from the authors' laboratory are given to show that lanthanide-binding metallopeptides, and now a full metallohomeodomain, can be generated by modular substitution of a Ca-binding EF-hand loop into the unrelated scaffold, the engrailed helix–turn–helix motif. We have previously shown that these peptides bind trivalent Ln(III) ions and promote DNA and phosphate hydrolysis, the targeted function. Here, a series of chimeric peptides are presented that differ only in the ninth loop position [given in parentheses; Peptides P3N (Asn), P3E (Glu), P3A (Ala), and P3W(D) (Asp)]. This residue, a putative second-shell ligand stabilizing a coordinated water, was found to influence not only metal affinity but also peptide folding. The affinity for Tb(III) was determined by Trp–Tb fluorescence resonance energy transfer and followed the order K_a = P3W(D) > P3A ≈ P3E > P3N. However, circular dichroism (CD) titrations with $EuCl_3$ showed that only P3W(D) and P3N folded to any extent upon metal binding, indicating that the Asp/Asn side chains stabilize the central loop structure and thus propagate folding of the peripheral helices, whereas neither Ala nor Glu appears to be interacting with the metal to organize the loop. Finally, we investigated the longer range context of a given loop substitution by cloning and expressing a lanthanide-binding homeodomain (C2), whose loop insertion sequence is analogous to that of peptide P3W(D). We find by CD that apo-C2 has a significant helical structure (∼25% α helicity), which increases further upon the addition of Tb(III) (∼32% α helicity). The protein's Tb(III) affinity is similar to that of the chimeric peptides. However, unlike previously reported metallopeptides, we find that EuC2 does not appreciably promote phosphate or DNA cleavage, which suggests a difference in metal accessibility in the context of the full domain. We have demonstrated that substituting β turns with metal-binding turns does not necessarily require homologous parental scaffolds or small flexible peptides but rather relies on the structural similarity of the motifs flanking the turn.

Introduction

To an inorganic chemist, the structural, spectroscopic, and mechanistic predictions of metal complex behavior are endlessly fascinating. A deeper understanding of metal complex reactivity helps both to explain observations and to establish new synthetic goals for generating systems of predictable function. The biological world, in particular, is a rich source of inspiration for many inorganic chemists, combining intricate biomolecular ligands and a surprising breadth of metal ions in reactive or structural roles. However, these biological systems are generally extremely complex. Along with the desire to deconstruct and understand specific natural systems comes the aspiration to tease out underlying, fundamental principles of bioinorganic function. This, in turn, opens the door to creating new function inspired by but not limited to nature's example.

Biomolecular design, still a relatively young field, offers the inorganic chemist a powerful tool toward the ambitious goal of addressing fundamental bioinorganic questions systematically. Designed proteins are often much simpler than the large, multicomponent enzymes they mimic, yet they retain significant structural and functional complexity. As such, these designed systems allow the bioinorganic chemist

* To whom correspondence should be addressed. E-mail: sonya-franklin@uiowa.edu.

10.1021/ic060877k CCC: $33.50
Published on Web 12/04/2006

to model enzyme function using native ligand sets in aqueous solution. Among the "big picture" questions in metalloenzymology that we are addressing through design are the following:

(1) How does the structural context of a metal site (in terms of flexibility, accessibility, charge, and sequence of flanking residues) influence activity?

(2) How is metalloenzyme activity tuned by the primary and secondary ligand sets?

(3) Are thermodynamically well-folded proteins and tight metal-binding sites related to "success" as an enzyme?

In this Forum Article, we will focus on the protein design method of modular turn substitution (also known as loop-directed mutagenesis) as it relates to addressing these fundamental tenants of biochemistry. We will provide examples from our laboratory showing that small peptides can be designed to bind both hydrolytically active metals and substrate (DNA) and that the reactivity, structure, and metal-binding affinity can be tuned in a predictable (and not so predictable) manner.[1] We also report here the first designed metallohomeodomains, thereby expanding our peptide design work to full protein domains and demonstrating that context of the loop substitution impacts both metal-affinity and hydrolytic activity. It is our hope that, along with the complementary set of articles in this Forum, these illustrations will highlight the flexibility and promise of biomolecular design in inorganic chemistry.

Strategies in Protein Design Using Native Scaffolds

Protein design can classically be considered to fall into two categories, namely, *de novo protein design* (true "from scratch" folded proteins) and *protein redesign* (based on a natural scaffold). The ability to write a sequence on paper and to subsequently create a folded helical bundle from this blueprint is a truly remarkable achievement (for a more detailed perspective on de novo design and its utility in inorganic chemistry, we refer you to the accompanying Forum Articles). However, here we will focus on the latter approach, which represents some of the earliest and most successful examples of manipulating protein structure and function to create new constructs.

Protein redesign takes advantage of the inherent stability of native proteins, the evolutionary flexibility of sequence variations, and the functional diversity of their natural states. The measure of "success" in a redesigned protein is dependent on the given scaffold, and this, in turn, must be chosen with the scientific goal in mind. General considerations for choosing a scaffold include (1) the native function of the scaffold (i.e., protein−protein interactions, ligand binding, DNA binding), (2) the inherent stability of the protein (including the difficulty of correctly folding disulfide bonds), (3) solubility and size, and (4) properties of the region to be modified.[2]

The scaffold, once chosen, can be modified in a number of ways. Interfaces can be changed by multiple point mutations on a surface or by alteration of several adjacent loop regions. In these cases, point mutations are often separated in the amino acid sequence but are nearby in the tertiary structure. This then creates an organized binding surface for a complementary partner, whether that is another protein, a target substrate, or a metal ion. Metalloproteins designed in this way continue to shed light on the factors involved in creating tight and selective binding for a variety of metal ions and clusters. For example, Regan designed both a rubredoxin analogue[3] and one of the earliest examples of de novo designed tetrahedral Zn-binding sites[4] into the IgG-binding B1 domain of the *Streptococcals* protein G, proving that grafted, solvent-exposed metal sites can exhibit significant affinity and ion selectivity. In another classic example, Skerra et al. also reported a solvent-exposed His_3 site built at the surface of the β-barrel protein retinol-binding protein, which was selective for Zn(II) over Cu(II) and Ni(II).[5] Also taking advantage of a protein with naturally variable loop regions, Sollazzo and co-workers describe a "minibody", a redesigned and abbreviated IG domain comprising the β-sandwich region of the V_H (heavy-chain variable) domain, and changes in the hypervariable H1 and H2 loops to generate a Zn-binding site.[6] Hellinga and co-workers have also generated a number of metalloproteins by modifying native scaffolds, basing the selection of residues mutated to create the binding site on computational predictions with the DEZYMER modeling program he developed.[7] Some classic examples from this prolific group include Zn biosensors,[8] designed models of the type III Cu_2 site of copper oxygenases[9] (both constructed on the maltose-binding protein scaffold), a non-heme iron superoxide dismutase model built on a thioredoxin scaffold,[10] and a $[4Fe-4S]^{2+/+}$ cluster binding site grafted onto one face of the small thioredoxin protein.[11] In all of these cases, residues adjacent in space but not concurrent in the primary structure were mutated to the desired ligand residues. The structure, metal-binding, cluster assembly and, in many cases, some reactivity of the target functions were achieved.

The above examples show that, with known tertiary structures and either computational modeling or combinatorial libraries, point mutations at surfaces can generate tight metal sites. Alternately, single loops can be modified or substituted by a "cassette" mutagenesis of a contiguous region of the amino acid sequence. In the simplest case, the scaffold presents the loop in a defined context and allows

(1) Franklin, S. J.; Welch, J. T. *Comments Inorg. Chem.* **2005**, *26*, 127.
(2) (a) Skerra, A. *J. Immunol. Methods* **2004**, *290*, 3. (b) Skerra, A. *J. Mol. Recognit.* **2000**, *13*, 167.
(3) Farinas, E.; Regan, L. *Protein Sci.* **1998**, *7*, 1939.
(4) Klemba, M.; Gardner, K. H.; Marino, S.; Clarke, N. D.; Regan, L. *Nat. Struct. Biol.* **1995**, 368.
(5) Schmidt, A. M.; Müller, H. N.; Skerra, A. *Chem. Biol.* **1996**, *3*, 645.
(6) (a) Bianchi, E.; Venturini, S.; Pessi, A.; Tramontano, A.; Sollazzo, M. *J. Mol. Biol.* **1994**, *236*, 649. (b) Pessi, A.; Bianchi, E.; Crameri, A.; Venturini, S.; Tramontano, A.; Sollazzo, M. *Nature* **1993**, *362*, 367.
(7) Hellinga, H.; Richards, F. M. *J. Mol. Biol.* **1991**, *222*, 763.
(8) Marvin, J. S.; Hellinga, H. *Proc. Natl. Acad. Sci. U.S.A.* **2001**, *98*, 4955.
(9) Benson, D. E.; Haddy, A. E.; Hellinga, H. W. *Biochemistry* **2002**, *41*, 3262.
(10) Pinto, A. L.; Hellinga, H. W.; Caradonna, J. P. *Proc. Natl. Acad. Sci. U.S.A.* **1997**, *94*, 5562.
(11) Coldren, C. D.; Hellinga, H.; Caradonna, J. P. *Proc. Natl. Acad. Sci. U.S.A.* **1997**, *94*, 6635.

the study of the given loop structure (i.e., as an immunogenic peptide) or clustered ligand set. Regan and co-workers showed in 1996 that loop expansion and/or swapping is well-tolerated (though stability is sacrificed with longer loops) by some well-folded native proteins such as the α-helical bundle *Rop*,[12] which opened the door to loop mutations for the purpose of manipulating function.

This modular cassette approach, which is in essence analogous to domain swapping and exon shuffling on a more local scale, has already generated a number of novel metal-binding sites in designed proteins (reviewed by Lu in 2001).[13] The single-loop-substitution approach is particularly suitable to the study of metal-binding sites because there are many examples of metal-binding regions in which the majority of the ligands are close together in the primary amino acid sequence. These include Zn-binding loops, such as that of astacin, a member of the metazincin family of peptidases (**H**Exx**H**xxGxx**H**),[14] in which three of the four amino acid ligands for Zn(II) occur within a short (≤11 aa) loop sequence. Alcohol dehydrogenase is an example of a Cys-coordinated Zn, also within a short loop (**C**GK**C**RV**C**x_7**C**), and many other Zn-binding proteins have at least two sequentially nearby residues with the **H**Exx**H** motif.[15] Cu-binding loops include the Cu(I) site of Atx1 (a copper chaperone; MT**C**SG**C**),[16] the prion protein octarepeat site (His side chain and Gly backbone amide N and O donors; P**HGG**GWGQ),[17] the type I sites of azurin (**C**TFPG**H**-SAL**M**) and plastocyanin (**C**SP**H**QGAG**M**), and the dimeric CuA site of cytochrome *c* oxidase (C*c*O; **C**SEL**C**GIN-**H**AY**M**).[18] Fe−S clusters commonly occur between two adjacent loops, such as in rubredoxin,[19] but also are coordinated to thiols of single loops in bacterial ferredoxins (such as *Clostridial* ferredoxin;[20] **C**IA**C**GA**C**). Finally, the Ca site of EF hands (**D**x**D**x**D**GxxDxx**E**)[21] is a ubiquitous example of a well-organized metal-binding loop and perhaps can even be considered a subset of the more general **D**x**D**x**D**G Ca-binding motif.[22]

Loop Mutations within Native Scaffolds

In recent years, many of the metal-binding loops mentioned above have begun to be put into new context through modular loop substitution onto native (or de novo designed) scaffolds. This has led to insights into redox chemistry, electron-transfer rates, folding, cooperativity, and enzymatic activity. We will briefly describe examples here and refer the reader to accompanying Forum Articles elaborating on these systems.

One striking example is the substitution of a CuA site for a CuB (type I, or blue copper) site, generating designed proteins that played an important role in unraveling the structural mysteries of the bimetallic CuA sites. Lu coined the phrase "loop-directed mutagenesis" to describe the substitution of a CuA loop from C*c*O into the analogous loop in azurin, a classic blue copper protein.[18] Both parental proteins have a Greek β-barrel scaffold, differing structurally primarily in the metal-binding loop. Thus, the mutation of the entire loop generated a very similar "purple CuA azurin". Because CuA sites often occur as one of several metal cofactors in electron-transfer proteins, the signature spectroscopic and reactivity profiles of the isolated CuA structure were extremely difficult to deconvolute. By placement of the CuA site into the same structural context as a type I blue copper site, the two could be individually studied and electron-transfer rates and potentials compared. These studies built on the work of van der Oost et al., who reported a loop substitution that correctly reconstructed the CuA site binding loop of C*c*O into a nonmetal-containing β-barrel (the CyoA subunit of cytochrome *o* quinol oxidase).[23] A range of similar Cu loop substitutions into analogous β-barrel structures have since been made by Lu and others,[24] and these systematic studies are teasing out subtle details about how the site is tuned to allow the entatic, or metastable, state required for fast redox kinetics in blue copper proteins. For a more detailed discussion of this design work, we refer the reader to the accompanying Forum Article by Lu.

In another example of the unique power of metalloprotein design, Yang and co-workers have used loop substitution to place a Ca(II) site into a nonnative scaffold, the small, β-strand-rich domain 1 of a cell adhesion protein, CD2.[25] Their goal was to create an isolated EF-hand Ca site to study the intrinsic metal-binding affinities of EF-hand loops. Because of the cooperative nature of Ca binding in native EF-hand proteins such as calmodulin, the intrinsic stability of the loops cannot be readily determined directly. In this case, poly-Gly linkers to either side of the Ca loop were required as "structural insulators" to provide the flexibility required to bind Ca(II) and Ln(III). Thus, they could isolate the loop from the influences of the protein context, with the protein matrix serving to drive the entropically demanding organization of the sequence as a loop, even in the apo form. The designed system allowed a unique comparison of loops in the absence of cooperativity, from which they concluded

(12) Nagi, A. D.; Regan, L. *Fold. Design* **1997**, *2*, 67.
(13) Lu, Y.; Berry, S. M.; Pfister, T. D. *Chem. Rev.* **2001**, *101*, 3047.
(14) Bode, W.; Gomis-Rüth, R.-X.; Stöcker, W. *FEBS Lett.* **1993**, *331*, 134.
(15) Vallee, B. L.; Auld, D. S. *Biochemistry* **1990**, *29*, 5647.
(16) Arnesano, F.; Banci, L.; Bertini, I.; Huffman, D. L.; O'Halloran, T. V. *Biochemistry* **2001**, *40*, 1528.
(17) Burns, C. S.; Aronoff-Spencer, E.; Dunham, C. M.; Lario, P.; Avdievich, N. I.; Antholine, W. E.; Olmstead, M. M.; Vrielink, A.; Gerfen, G. J.; Peisach, J.; Scott, W. G.; Millhauser, G. L. *Biochemistry* **2002**, *41*, 3991.
(18) Hay, M. T.; Richards, J. H.; Lu, Y. *Proc. Natl. Acad. Sci. U.S.A.* **1996**, *93*, 461.
(19) Holm, R. H.; Kennepohl, P.; Solomon, E. I. *Chem. Rev.* **1996**, *96*, 2239.
(20) Gao-Sheridan, H. S.; Pershad, H. R.; Armstrong, F. A.; Burgess, B. K. *J. Biol. Chem.* **1998**, *273*, 5514.
(21) Falke, J. J.; Drake, S. K.; Hazard, A. L.; Peersen, O. B. *Quart. Rev. Biophys.* **1994**, *27*, 219.
(22) Rigden, D. J.; Galperin, M. Y. *J. Mol. Biol.* **2004**, *343*, 971.
(23) van der Oost, J.; Lappalainen, P.; Musacchio, A.; Warne, A.; Lemieux, L.; Rumbley, J.; Gennis, R. B.; Aasa, R.; Pascher, T.; Malmström, B. G.; Saraste, M. *EMBO J.* **1992**, *11*, 3209.
(24) (a) Buning, C.; Canters, G. W.; Comba, P.; Dennison, C.; Jeuken, L.; Melter, M.; Sanders-Loehr, J. *J. Am. Chem. Soc.* **2000**, *122*, 204. (b) Yanagisawa, S.; Dennison, C. *J. Am. Chem. Soc.* **2004**, *126*, 15711. (c) Hwang, H. J.; Berry, S. M.; Nilges, M. J.; Lu, Y. *J. Am. Chem. Soc.* **2005**, *127*, 7274.
(25) Ye, Y.; Lee, H.-W.; Yang, W.; Shealy, S.; Yang, J. J. *J. Am. Chem. Soc.* **2005**, *127*, 3743.

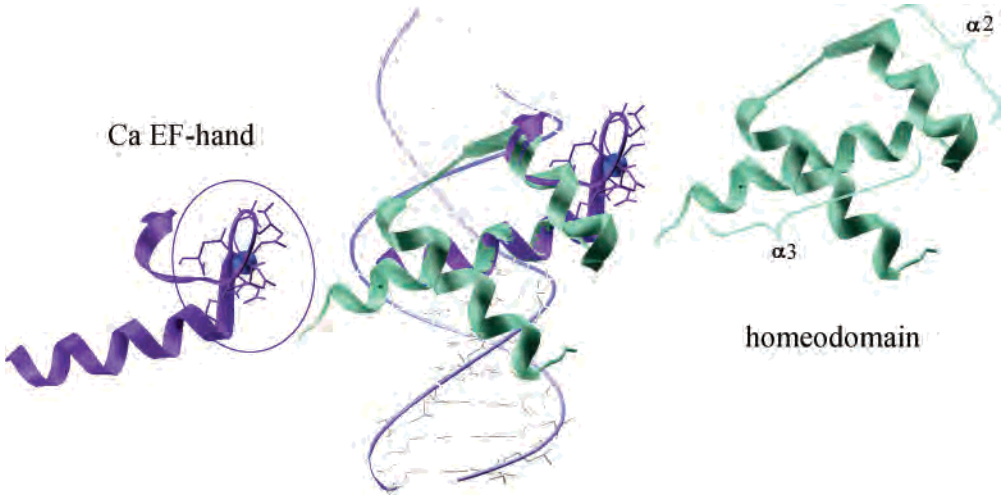

Figure 1. Structural similarities of a single EF-hand motif of *calmodulin* (1OSA; purple) and the HTH motif of *engrailed* homeodomain (1ENH; green) highlighted in an overlay of known crystal structures (center). Our designed chimeric peptides comprise the Ca/Ln-binding turn (circled in purple, left) and the helices of the DNA-binding motif (α2 and α3 in green, right).

that both the number of negatively charged ligands and the careful screening of the anionic ligand−ligand repulsion by cationic loop residues are the determining factors in intrinsic loop stability.

Although not a native scaffold as in the above examples, modular loop substitution into well-characterized and well-folded de novo designed helical bundles has also been reported. Examples from the Dutton[26] and Holm[27] laboratories incorporated $[4Fe-4S]^{2+/+}$ clusters into the loop between adjacent helices, for specific electron-transfer reactions with either iron(II/III) heme or adjacent Ni(II) centers, respectively, within the bundle. The Gibney laboratory has reported using these types of small Cys-rich loop peptides to explore Co(II) and Zn(II) binding as well as $[4Fe-4S]^{2+/+}$ clusters[28] (see also the accompanying Forum Article elaborating on these studies). Using these minimalist systems as models of redox-active metalloproteins is conceptually related to pursuing small-molecule synthetic analogues of active sites, a staple of bioinorganic chemistry in understanding enzyme function. However, the loop-substituted designs with their addition of controllable variables such as protein architecture, folding, solvent accessibility, and metal center distances allow the systematic deconstruction of the spectroscopy and electronics of these involved, multi-centered proteins.

A recent report by Park et al. demonstrates the remarkable extent that loop substitution can be taken toward redesigning novel metalloprotein enzymes.[29] The combination of loop insertion, deletion, and substitutions to reconstruct the surface of one protein (the $\alpha\beta-\beta\alpha$ scaffold glyoxalase II), followed by point mutations to optimize stability and activity, allowed the conversion of glyoxalase activity to β-lactamase activity. Although both proteins have the $\alpha\beta-\beta\alpha$ fold and a Zn_2 active site that catalyzes the hydrolysis of the target bond, the substrate targets are significantly different sterically and electronically. This extensive reconstruction illustrates the emerging directions of metalloprotein design.

Active-Site Context and Metalloprotein Design

To a first approximation, an inorganic chemist can predict the spectroscopy and reactivity of a given metal complex by knowing the metal ion and donor-atom set. However, remarkable subtleties in coordination geometry and electronics lead to huge variations in reactivity and function. Certainly, this is true in bioinorganic systems as well, where similar active sites are generally supposed to access similar chemistry. However, a recurring theme in bioinorganic chemistry is that the same active site can, in different contexts, have a range of activities within a given functional palette. Just as a mother cat can both gently carry a kitten and effectively dispatch a rat with the same jaws, context influences function in proteins as well (for example, hemoglobin carries O_2, whereas cytochrome P-450 splits and activates O_2). A minimalist designed system is an ideal way to investigate the role of the protein matrix in delivering, orienting, constraining, and electronically tuning the active site. By using the "modular-turn-substitution" approach to incorporate loops into known scaffolds, we can directly address the impact of context on the metal-binding loop.

We set out to design an enzyme, specifically, a nuclease, as a test case to investigate context in tuning structure and function in metal-binding sites of proteins.[1,30,31] A successful nuclease must be able both to bind and cut DNA, and thus two functions must be accommodated by the same protein matrix. Our approach was to incorporate a structural Ca-binding site (the EF-hand) into a topologically similar turn from an unrelated motif [the helix−turn−helix (HTH) DNA-binding motif]. Both motifs are examples of the $\alpha-\alpha$ corner

(26) Gibney, B. R.; Mulholland, S. E.; Rabanal, F.; Dutton, P. L. *Proc. Natl. Acad. Sci. U.S.A.* **1996**, *93*, 15041.
(27) Laplaza, C. E.; Holm, R. H. *J. Am. Chem. Soc.* **2001**, *123*, 10255.
(28) Kennedy, M. L.; Gibney, B. R. *J. Am. Chem. Soc.* **2002**, *124*, 6826.
(29) Park, H.-S.; Nam, S.-H.; Lee, J. K.; Yoon, C. N.; Mannervik, B.; Benkovic, S. J.; Kim, H.-S. *Science* **2006**, *311*, 535.
(30) Kim, Y.; Welch, J. T.; Lindstrom, K. M.; Franklin, S. J. *J. Biol. Inorg. Chem.* **2001**, *6*, 173.
(31) Welch, J. T.; Sirish, M.; Lindstrom, K. M.; Franklin, S. J. *Inorg. Chem.* **2001**, *40*, 1982.

Figure 2. Sequences of de novo designed chimeric peptides and metallohomeodomain C2. The parental *engrailed* sequence is given in green, with the excised turn in blue. The three helices of *engrailed* are shaded. The EF-hand Ca-binding loop (purple) and, in some cases, flanking sequences from *calmodulin* (black) were inserted into the HTH motif in various orientations. The numbering scheme indicates flanking residues before (−1) and after (+13) the Ca loop (+1 through +12). For the last four peptides, the 9th position of the loop, a putative second-shell interaction with coordinated water, was varied to test the impact of this residue on metal affinity and folding (red).

supersecondary structure, which describes a 90° turn between helices.[32] Figure 1 shows the overlay of the two turns, using fragments of known crystal structures to illustrate the collinearity of the helices in the motifs.

We designed a series of peptides via modular turn substitution of these α−α corners (Figure 2). The parental HTH motifs were taken from either *engrailed* or *antennapedia* homeodomain sequences and the Ca loops from either *calmodulin* (bovine CaM, EF-hand 1 or 3) or the consensus EF-hand sequence. The loops were inserted by matching residues in 3-dimensional space at the entrance and exit of the loop (see Figure 1) and varied to test the modular-turn-substitution approach. These first-generation designs had mixed success using the metric of structure,[30,33] although all did bind metal ions [Ln(III)] with low micromolar affinities, and were able to promote DNA or phosphate hydrolysis, the targeted function (for a more complete review, see ref 1).

The extent of folding upon metal binding illustrated two critical issues of loop context in the HTH system: (a) the length of the loop insert, or how much "turn" to excise, and (b) the identity and position of the flanking residues that anchor the helix termini at the turn "pivot" (the contact point between 90° helices). The HTH is a relatively tight turn of only four residues, which has specific hydrophobic contacts between the turn and adjacent helices to promote the fold.[34] These include a highly conserved Trp residue in helix 3 (i.e., W48 of *engrailed*), nearly universally conserved in homeodomains.[35] The loop replacing the turn, in contrast, is larger and unstructured in the absence of metal ions, and indeed none of the peptides have organized secondary structure in the apo state. Upon binding Ln(III) or Ca(II) ions, some of the peptides fold to a classic α−α corner. The thermodynamically favorable metal binding in essence pays the entropic cost of folding the turn, thereby bringing the pivot point of the turn together. Provided the intersection of the two nacent helices has specific favorable interactions at this corner, further stabilization and nucleation of the helices on either side occurs.

We explored a variety of loop lengths, positions, and flanking residues and reached these conclusions for loop context in HTH substitutions:

(1) Hydrophobic contacts at specific positions before and after the EF-hand loop must be retained, by the deliberate coincidence of key hydrophobic residues of the two parental turn motifs. Hydrophobic contacts at −1, +13, and +16 relative to the EF-hand loop (+1 through +12) are critical. Omitting the hydrophobic contact at +13 (peptide P5) or at +16 (peptide P5b) resulted in poor folds.

(2) Omitting Trp at +16 (through a Trp → His mutation; peptide P3) compromised the HTH structure of the motif.

(3) The best location for turn substitution into the HTH involves a longer N-terminal helix and a shorter C-terminal helix. Turns inserted with a register shift of one helical turn (four residues) to the N terminus did not fold well (for example, peptide P4a vs P3W).

Of the peptides tested, peptide P3W (Figure 2) was the best-folded example upon binding trivalent lanthanides, reaching a maximum helical content of ∼38% helicity (compared to the predicted value of 48%), based on mean residue ellipticity at 222 nm [Θ_{222}] under saturating metal conditions ($EuCl_3$ in Tris, pH 7.8).[36] In fact, La^{III}P3W was well-enough organized to complete an NMR solution structure based on nuclear Overhauser effect spectrometry (NOESY) integrations.[36] The ^{1}H NMR spectrum was nicely dispersed, indicating a folded structure upon the addition of La(III). Paramagnetic ion substitutions with Eu(III) and Yb(III) ions helped to confirm the binding site location because of paramagnetic broadening exclusively in the binding loop. The diamagnetic LaP3W 2D spectra were fully assigned, and chemical shifts of backbone amide protons[37] indicated that the metallopeptide adopted the predicted helix−loop−helix secondary structure. A DYANA structural model was constructed based on NOE-derived constraints. The model showed that the metallopeptide adopts a classic helix−loop−helix EF-hand structure,[36] with somewhat disordered helical termini as expected of isolated peptides. One notable difference from the EF hands in native *calmodulin* was the position of Asp17, the 9th position of the loop (Figure 2), which in *calmodulin* is involved in a hydrogen bonding with coordinated water. In the LaP3W structure, this Asp side chain was best modeled in a more open position, pointing away from the metal center, though a minor population of the carboxylate side chain pointing toward the metal center was also supported by some DYANA solutions. Because

(32) Efimov, A. V. *FEBS Lett.* **1996**, *391*, 167.
(33) Sirish, M.; Franklin, S. J. *J. Inorg. Biochem.* **2002**, *91*, 253.
(34) (a) DeGrado, W. F.; Summa, C. M.; Pavone, V.; Nastri, F.; Lombardi, A. *Annu. Rev. Biochem.* **1999**, *68*, 779. (b) Efimov, A. V. *FEBS Lett.* **1984**, *166*, 33.
(35) Banerjee-Basu, S.; Moreland, T.; Hsu, B. J.; Trout, K. L.; Baxevanis, A. D. *Nucleic Acids Res.* **2003**, *31*, 304.
(36) Welch, J. T.; Kearney, W. R.; Franklin, S. J. *Proc. Natl. Acad. Sci. U.S.A.* **2003**, *100*, 3725.
(37) Wishart, D. S.; Bigam, C. G.; Holm, A.; Hodges, R. S.; Sykes, B. D. *J. Biomol. NMR* **1995**, *5*, 67.

LaP3W is a monomer in solution, as shown by static light-scattering experiments,[36] the loop is apparently more flexible than that in the native context, wherein this portion of the loop is constrained as a short β strand by back-to-back dimerization of the EF-hand motifs. As we will discuss below, the second-shell interaction between the 9th loop position and the metal is still of some importance in the coordination behavior of the loop.

These structural studies showed that a designed peptide that retains the correct insert register, hydrophobic contacts (including the conserved Trp), and loop length can successfully accommodate a metal-binding loop from an unrelated fold into a new motif scaffold. Furthermore, we were able to demonstrate that these Eu(III) metallopeptides promoted phosphate and DNA hydrolysis, and, importantly, the rates of cleavage were 10−100-fold faster than that of free ion (or more accurately, buffer-associated metal ions, due to weak Eu^{III}Tris complexes).[30] The hydrolysis occurred with modest sequence preference, which suggests that a folded metallopeptide is interacting with the DNA groove.[1,36,38]

Local Context: Second-Shell Interactions within the Active Site

By combining metal-binding and DNA-binding functions via modular turn substitution, we were able to create novel, reactive peptide-based nucleases. This provides us a minimalist model system for hydrolytic function and thus allows us to look at the local context of the metal site in greater depth to address how proteins tune the reactivity of an active site. In native metalloenzymes, there is generally a tightly regulated cascade of hydrogen bonds, organized water molecules, and hydrophobic pockets or channels that direct and control the reactivity by modulating the electronics of the metal center or altering its accessibility to the substrate. One classic example is the tuning of the Zn Lewis acidity in the active site of carbonic anhydrase, which Fierke and co-workers nicely demonstrated with a series of point mutations near the metal center.[39] In this system, the loss of critical second-shell hydrogen-bonding interactions results in a decrease in the Zn-binding affinity as well as enzymatic reaction rates. Notably, the loss of the indirect ligand Thr199 that accepts a hydrogen-bond from Zn-bound water reduced the Zn(II) affinity by approximately 1 order of magnitude. Both the primary ligands and the neighboring residues affect the electronic character of the Zn(II) ion, which is, in turn, reflected in coordinated water pK_a values and enzyme reaction rates.

We wished to test this affect in a designed hydrolytic "enzyme", as a measure of our success in mimicking function. Using loop-substituted designed nucleases, we can isolate several factors in the complex hydrolysis story, namely, the impact of a neighboring second-shell ligand on metal binding, loop stability, and enzymatic activity. With our chimeric peptides, the active-site "pocket" is relatively exposed, so substrate accessibility is not a limiting factor (although we will find that context matters for this issue, too, when considering full domains, *vide infra*). Here, we began by addressing how the second shell impacts the metal-binding affinity.

Because the metallopeptide LnP3W was a success in terms of folding a small motif, we elected to use this starting point to investigate the role of second-shell ligands on metal binding and, eventually, on reactivity. Along with P3W, three peptide analogues were prepared to explore the role of position 9 of the loop (residue 17 of the peptides, indicated in red in Figure 2), a putative hydrogen-bonding interaction with coordinated water. The NMR structure of LaP3W showed that this outer-sphere interaction is likely a transient hydrogen bond rather than a more directional, constant contact.[36] Nonetheless, our comparison of water pK_a values in the first-generation peptides (P3W, P4a, and P5b) by Eu luminescence spectroscopy[40] suggested that this residue does influence the Lewis acidity and metal affinity of the site. However, these peptides were quite different in sequence and structure, as was already discussed, making direct comparisons difficult.

By generating a series of P3W analogues that differ in only one residue, we can isolate the effect of this side chain in a known context [note that, for this discussion, we will designate P3W as P3W(D) to highlight the amino acid of interest (D_{17}) in the original peptide]. We manually synthesized the peptides using standard fluorenylmethoxycarbonyl (Fmoc) solid-phase coupling chemistry, followed by high-performance liquid chromatography (HPLC) purification. Coupling and deprotections were monitored at each step, which uncovered a few particularly difficult coupling steps (T_1E_2, $T_{15}I_{16}$, and R_3R_4, for example) that may have contributed to the challenges faced with automated synthesis of these types of sequences in the past (unpublished results). Peptide purity and identity were confirmed by mass spectrometry.

In P3W(D), the 9th loop position is Asp, an anionic, hydrogen-bond acceptor. We additionally prepared P3A, P3E, and P3N with the indicated mutations at the 9th position. In *calmodulin*, where the loop is more rigidly constrained by motif dimerization, this position has been shown to be highly influential in metal-exchange kinetics and binding affinities and has therefore been designated the "gateway position" of the EF-hand motif.[21] When the gateway position in *calmodulin* is occupied by Asp (the consensus residue), hydrogen bonding to the coordinated water stabilizes this structure, whereas the longer Glu side chain has been found to bind directly to the metal, displacing a water molecule. Thus, with these peptides, we sought to determine the impact of the residue charge (Asp vs Asn), size (Asn vs Ala, both neutral), and side-chain length (Asp vs Glu) on metal binding in these isolated, monomeric, EF-hand-like systems.

The binding affinities of the four peptides for Tb(III) were determined by fluorescence titration, by exciting into the

(38) Wong-Deyrup, S. W.; Kim, Y.; Franklin, S. J. *J. Biol. Inorg. Chem.* **2005**, *11*, 17.

(39) DiTusa, C. A.; McCall, K. A.; Christensen, T.; Mahapatro, M.; Fierke, C. A.; Toone, E. J. *Biochemistry* **2001**, *40*, 5345.

(40) Jain, S.; Welch, J. T.; Horrocks, W. D., Jr.; Franklin, S. J. *Inorg. Chem.* **2003**, *42*, 8098.

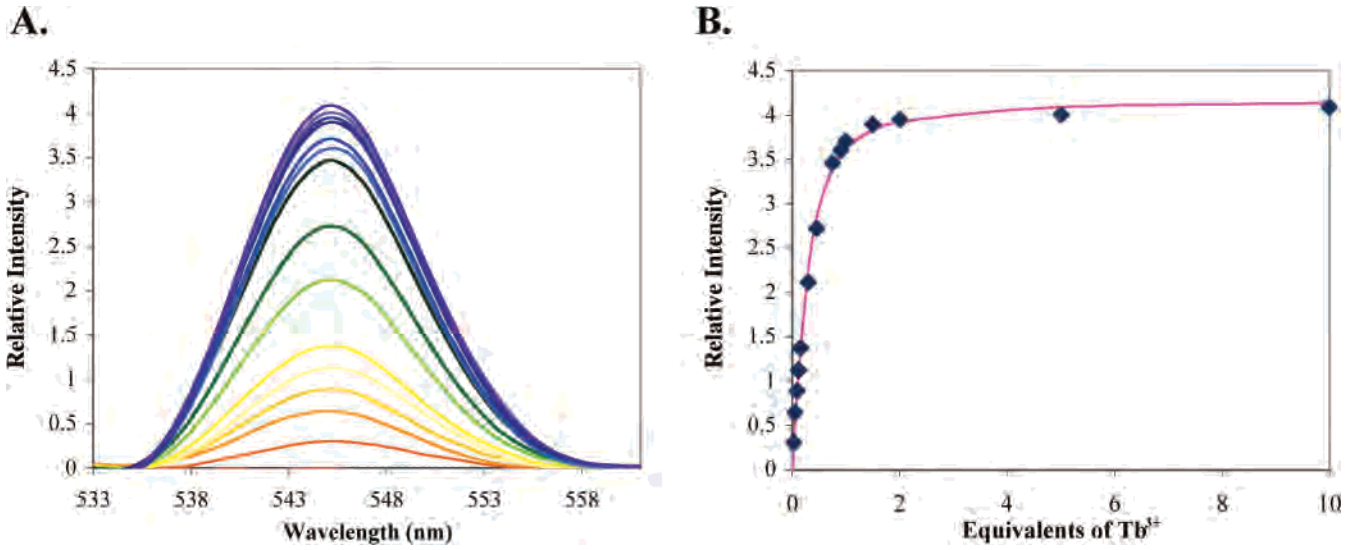

Figure 3. Titration of representative peptide P3W(D) with $TbCl_3$, followed by Tb(III) fluorescence spectroscopy (FRET). Samples containing 30 μM peptide in a 10 mM HEPES buffer at pH 6.9 were titrated with up to 10 equiv of Tb. The $TbCl_3$ stock solution contained 30 μM peptide to maintain a constant peptide concentration throughout the titration. Samples were excited at 290 nm (Trp band), and emission at 545 nm was observed following energy transfer from Trp to Tb(III). (A) Tb(III) excitation spectra (peak growing in). (B) Emission intensity at 545 nm vs equivalents of Tb(III) and a fit to 1:1 association (as in ref 29).

Table 1. Tb-Binding Affinities of Chimeric Peptides and Metallohomeodomain C2 (10 mM HEPES Buffer, pH 6.9)[a]

chimera	Tb(III) K_d (μM)	chimera	Tb(III) K_d (μM)
P3W(D)	4.2 ± 0.5	P3E	10.6 ± 0.5
P3N	17.0 ± 3.3	C2	8.7 ± 2.1
P3A	11.4 ± 2.6		

[a] Conditional affinities were determined by Trp-Tb FRET, and reported errors are standard deviations of three measurements.

single Trp band at 290 nm (W_{24}) and following the emission of Tb(III) at 545 nm. A 495-nm band-pass filter was included to edit the direct emission of Trp. Because the observed Tb-based emission is generated by energy transfer from the excited Trp, this method is a sensitive reporter of Tb(III) ions interacting with Trp residues within approximately 10 Å.[25]

Figure 3 shows the Tb emission spectra and the resultant intensity as a function of added $TbCl_3$ for representative peptide P3W(D). The data for each peptide were nicely fit to a 1:1 association model as described in ref 25, although the inclusion of additional nonspecific sites in the model did not improve the fit. The peptides bind 1 equiv of Tb(III), with low micromolar affinities (Table 1). It should be noted that similar values were determined by direct observation of the Trp emission (data not shown), the intensity of which decreases as a function of added metal. This decrease in Trp emission is seen in wild-type *engrailed* homeodomains because it folds as well.[41]

It is clear from the data in Table 1 that the putative second-shell interaction between loop position 9 and the metal (either indirectly through bound solvent or directly) does impact the affinity of the site of the mid-sized lanthanide ion Tb-(III). The most notable difference is between P3W(D) and P3N, which differ in only a functional group, taking the carboxylate of Asp to the amide of Asn. The resultant change in charge (negative to neutral) and potential role (charged hydrogen-bond acceptor to either neutral acceptor or donor) apparently results in a less favorable metal-binding site, with the Tb(III) affinity destabilized by approximately 3.6 kJ/mol, equivalent to a very weak hydrogen bond.[42] This is a small effect in terms of the metal affinity were it a direct contact but is not insubstantial for a second-shell interaction, wherein the hydrogen bond stabilizes a metal ligand (water).[39,43]

In comparison, P3A removes the hydrogen-bond acceptor entirely and also removes some steric bulk around the metal center. Thus, solvent exchange and hydrogen bonding with a bulk solvent (rather than specific second-shell interactions with a peptide side chain) is more readily available. The loss of the favorable Asp $\rightarrow$ H_2O interaction in P3W(D) costs $\sim$2.5 kJ/mol of Tb(III)-binding affinity, but the "hole" in the coordination shell and accessible solvent hydrogen bonding are apparently slightly more favorable than the neutral Asn $\rightarrow$ H_2O interaction. P3E has essentially the same affinity for Tb(III) as P3A does, suggesting that the longer Glu side chain may neither be directly ligating the Tb(III) nor be aligned efficiently to help stabilize the first-shell water molecule. Determination of the hydration number for the various (Eu) metallopeptides will help to address whether P3E has the same open site for solvent as P3A or whether the similarity in the binding affinities arises from other coincidences.

An investigation of the structure of these four peptides as a function of metal-binding further illustrated the importance of the subtle stabilizing influence of the gateway position on the loop structure and thus the overall peptide fold (Figure

(41) Stollar, E. J.; Mayor, U.; Lovell, S. C.; Federici, L.; Freund, S. M. V.; Fersht, A. R.; Luisi, B. F. *J. Biol. Chem.* **2003**, *278*, 43699.

(42) Desiraju, G. R. *Acc. Chem. Res.* **2002**, *35*, 565.

(43) It should be noted that here we are defining "second-shell interactions" as the electronic, steric, and structural component to metal binding that is dependent on the gateway residue. This includes long-range coordination effects through water, although it is likely that these may be transient in some cases.

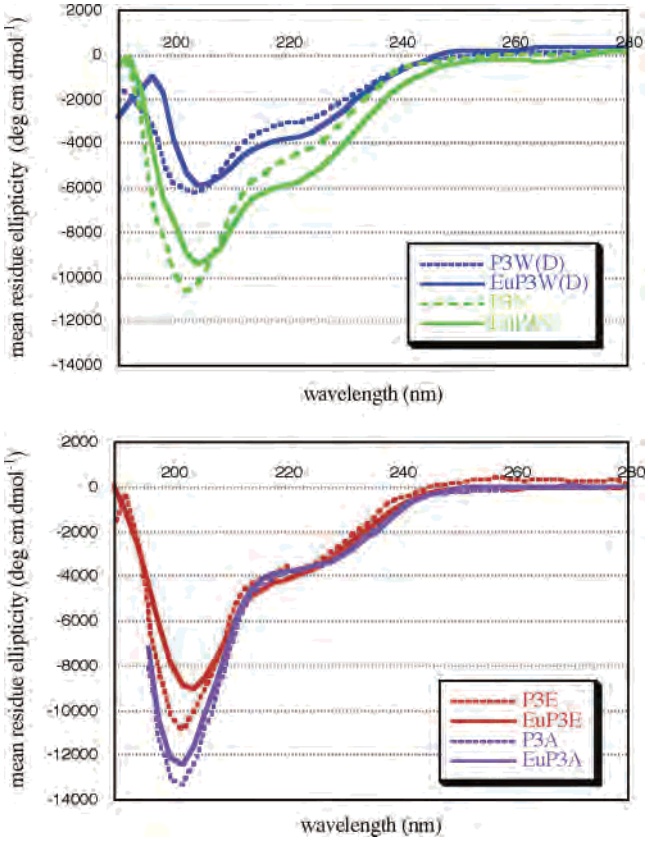

Figure 4. CD spectra of chimeric peptides in the presence (solid) and absence (dashed) of equimolar $EuCl_3$, in a 20 mM Tris buffer, pH 7.2.

4). Circular dichroism (CD) spectroscopy of EuP3W had previously shown peptide P3W(D) to have increased helical structure upon metal binding.[31,36] Because the three peptide analogues P3E, P3A, and P3N maintained the key hydrophobic contacts and loop insert register of P3W, we expected the three peptides to have metal-dependent folding behavior similar to that of P3W(D). However, only P3N showed any increase in the helical structure in the presence of lanthanide ion (as evidenced by an increase in the negative band at 222 nm). EuP3A had no more long-range structure than apo-P3A, and EuP3E showed only a small red shift in the band near 204 nm, indicative of maintaining primarily random-coil structure. We have evidence from both Trp fluorescence studies with Eu(III)[30,31,36] and the Trp−Tb fluorescence resonance energy transfer (FRET) studies reported here that at very least the loop region of these designed peptides fold upon binding middle lanthanides Eu(III) and Tb(III), bringing the single Trp (W_{24}) nearer the metal and causing changes in the emission of the fluorophore. Therefore, we conclude that although the loop folds to bind metal, the nucleation of helicity is highly dependent on the stability or flexibility of the metal loop.[44] An available hydrogen-bonding contact at the gateway position (Asp or Asn at position +9) is apparently a key factor in stabilizing the loop and, consequently, long-range structure.

(44) Estimates of the helical content under these experimental conditions showed only modest α helicity (12−19%).

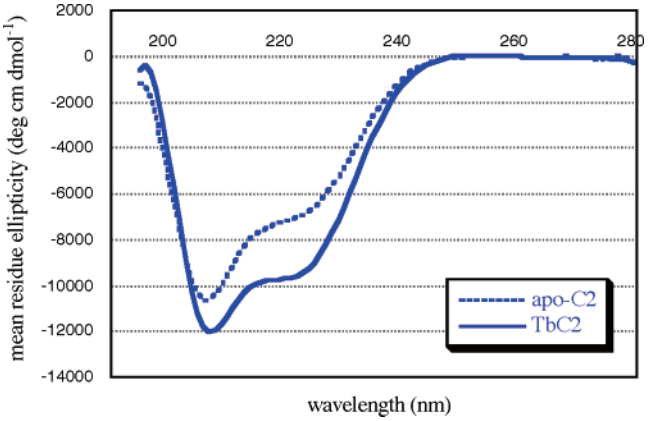

Figure 5. CD spectra of chimeric homeodomain C2 in the presence (solid) and absence (dashed) of equimolar $TbCl_3$, in a 10 mM HEPES buffer, pH 6.9.

How Domain Context Impacts Folding and Affinity

In our previous work, we found that the concept of swapping a metal-binding turn into a completely unrelated turn within supersecondary structures was viable but that folding of the motif is heavily dependent on the location of the turn and the presence of the metal to nucleate the fold. This is a recurring theme in peptide−metal interactions because folding involves an enthalpic and entropic balance between many subtle internal and solvation contacts. The chimeric peptides have proven to bind metals and (in some cases) adopt supersecondary structure as designed, but they are necessarily more "open" and flexible than the full parental domain with three helices. To model more complex metalloenzyme behavior, including subtleties of domain folding, flexibility, and substrate recognition, correct insertion of a metal site into a full protein is necessary. We therefore wished to compare the affinity and function of loop substitution within the context of the entire homeodomain to those of the same loop substitution in a smaller peptide framework.

A critical benchmark for our design approach is succeeding in creating a folded metallohomeodomain. To explore the impact of binding-site context within a global fold, we incorporated the chimeric (substituted) HTH sequence represented by P3W into the full engrailed homeodomain by loop mutation into *engrailed*. Using standard molecular biology techniques, we designed, cloned, expressed, and purified a series of loop-substituted chimeric *engrailed* derivatives.[45] We find that the designed protein C2 (Figure 2) meets this criterion, representing the extrapolation of the modular-turn-substitution approach of two physiologically unrelated motifs into the tertiary domain. As shown in Figure 2, peptide P3W is a subset of the sequence of C2, and thus we can compare directly binding and reactivity as a function of long-range context.

The structure of C2 was investigated by CD spectroscopy, in both the presence and absence of the trivalent lanthanide Tb. As shown in Figure 5, apo-C2 has significant α-helical character (~25% helicity), showing a propensity to adopt a helical bundle structure even without the metal. This is a

(45) Lim, S.; Franklin, S. J. *Protein Sci.* **2006**, *15*, 2159.

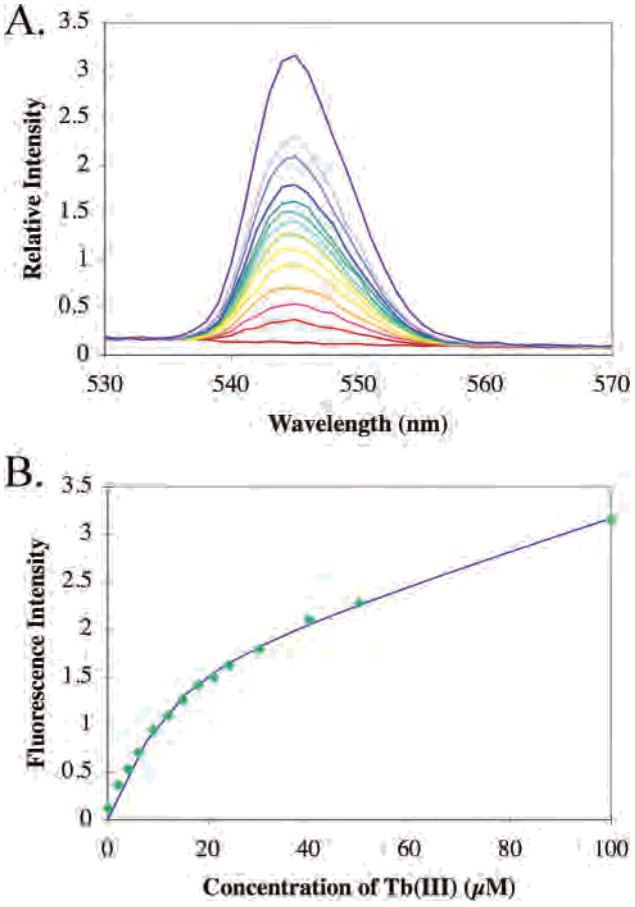

Figure 6. Titration of apo-C2 with $TbCl_3$, followed by Tb(III) fluorescence spectroscopy (FRET). Samples containing 10 μM C2 in a 10 mM HEPES buffer at pH 6.9 were titrated with up to 10 equiv of Tb. The $TbCl_3$ stock solution contained 10 μM C2 to maintain a constant protein concentration throughout the titration. Samples were excited at 290 nm (Trp band), and emission at 545 nm was observed following energy transfer from Trp to Tb(III). (A) Tb(III) excitation spectra (peak growing in). (B) Emission intensity at 545 nm vs Tb(III) concentration and a fit to a strong 1:1 association with a second weak affinity site (as in ref 29).

significant difference from the peptides, which have no organized secondary structure in the absence of metals. However, the addition of Tb(III) substantially further increases helicity (to ~32% helicity), as was the case for the peptides, and a similar effect is seen with other trivalent lanthanides as well.[45] The organization of the loop in the holoprotein appears to propagate helical structure adjacent to the binding site but may also alter favorable contacts present in the apo structure. Overall, the CD spectrum shows that the secondary structure characteristics of TbC2, a mix of extended structure and α helicity, mimics that of wild-type *engrailed* strongly.[46] Ongoing NMR structural studies of LaC2 have verified that C2 adopts a local secondary structure very reminiscent of *engrailed*.[47]

As with P3W, the transfer of energy from Trp to nearby Tb(III) leads to an increase in Tb emission at 545 nm, which can be well-modeled with a 1:1 association of Tb(III) and protein (Figure 6). For C2, an additional, nonspecific Tb-binding interaction was included in the fit. This additional component may be due to either nonspecific collisional quenching, weakly associated Tb(III) ions interacting with the very basic protein, or a very broad folding curve. Thermal denaturation studies show that the transition from folded to unfolded is very broad for metalated C2 (manuscript in preparation), suggesting that there are regions of the protein that fold upon Tb binding without cooperatively organizing the entire domain. This broad folding curve may be reflected in a range of apparent Tb(III) affinities in the titration because the fluorescence technique reports only on Tb−Trp distances, which may vary significantly as the protein folds.

Interestingly, the affinity of C2 for Tb(III) under these buffer and pH conditions is $K_d = 8.7 \pm 2.1$ μM, slightly weaker than that observed for the identical chimeric HTH/EF-hand loop afforded by peptide P3W(D). Clearly, there is a significant protein-folding component to the thermodynamic stability of metal binding in both peptide and protein because the tertiary structure is unstable in the absence of metal in both cases. However, the similarity of the binding constants in the isolated HTH peptide and the full homeodomain seems to indicate that the local structure of the metal loop is not significantly hindered or helped by a longer-range protein structure during metalation of C2.

Domain Context and Reactivity

The design of small peptides as enzyme mimics gave us a starting point for testing the general principles of tuning active-site reactivity. We found that our chimeric peptides promoted DNA hydrolysis, a fairly difficult reaction with an uncatalyzed rate recently reestimated to have a half-life of 30 million years.[48] We observed that even those peptides that did not fold substantially (EuP4a and EuP5b) enhanced hydrolysis of DNA and model phosphate esters bis(nitrophenyl) phosphate (BNPP) and nitrophenyl phosphate (NPP).[33] The cleavage was first order in substrate (BNPP) and in metallopeptide (though less than 10 turnovers are observed; unpublished results).

We were therefore interested in whether the Ln loop was equally reactive in the chimeric peptides and the full metallohomeodomains. We compared the rate of cleavage of both the diphosphate (BNPP) and monophosphate (NPP) ester substrates by EuP3W and by EuC2, which have an insertion context and sequence identical with those of the EF-hand loop. Intriguingly, while EuP3W cleaved these small substrates and DNA,[35] there was no observable phosphate hydrolysis over the background by EuC2. EuC2 was also unreactive toward plasmid DNA, although cleavage of very specific target sites may not be readily observed with the simple supercoiled to nicked plasmid assay. Determining the target binding site(s) of LnC2 will be necessary to rule out cleavage at high affinity sites.

The somewhat surprising result that EuC2 is substantially unreactive shows that domain folding and metal-site access dramatically impact the reactivity of the metal, even when the primary structure and local supersecondary structure are

(46) Clarke, N. D.; Kissinger, C. R.; Desjarlais, J.; Gilliland, G. L.; Pabo, C. O. *Protein Sci.* **1994**, *3*, 1779.
(47) Lim, S.; Franklin, S. J. **2006**, in preparation.
(48) Schroeder, G. K.; Lad, C.; Wyman, P.; Williams, N. H.; Wolfenden, R. *Proc. Natl. Acad. Sci. U.S.A.* **2006**, *103*, 4052.

retained. With the folded domain, we now have a starting point to begin to reintroduce reactivity by manipulating the accessibility of the lanthanide site.

Outlook for Metalloenzyme Design

Simultaneously creating active, folded, and selective metalloproteins by grafting metal sites into a functional scaffold is a substantial task. The examples of HTH/EF-hand chimeras from our group have again illuminated the challenges involved in the protein design of functional metalloenzymes. We found that an indirect, second-shell ligand within the loop influences metal affinity, with the anionic Asp stabilizing the Tb(III) site by ~3.6 kJ/mol over the neutral, but sterically similar, Asn residue. Removing the side-chain hydrogen-bond acceptor entirely by substituting the much smaller Ala residue was actually modestly more favorable for Tb(III) binding than the neutral Asn residue but compromised the metal-dependent helical structure of the peptide. The longer Glu side chain also appeared not to be interacting with the metal, as either a direct or indirect (hydrogen-bonding) ligand, because P3E had a metal affinity similar to that of P3A and also had little impact of metal complexation on the global structure. Somewhat surprisingly, this indirect ligand is a factor in peptide folding: the size-selected Asn or Asp second-shell ligand appears to be critical to the metal-dependent structure, even though in the case of P3N the thermodynamic cost of organizing the loop to bring the HTH "core" together results in a weaker metal affinity. The apparent absence of this indirect contact in P3E and P3A fails to provide stabilization of the putative β strand across the loop (residues 7−9 of the loop), and thus Tb(III) binding by the EF-hand sequence is likely neither entropically favored by preorganization nor penalized by constraining the loop's degrees of freedom.

In this work we also compared the identical chimeric turn substitution sequence within the context of a full homeodomain to that of the simple HTH peptide (essentially half the domain). In the case of the larger domain C2, we found that the thermodynamic price of folding the full domain resulted in a similar (or slightly weaker), rather than a stronger, lanthanide ion affinity relative to the flexible peptide analogue. This may be due to the apoprotein having favorable secondary and tertiary contacts that are altered upon metal binding, whereas apopeptide P3W(D) had no preorganized structure to disrupt. Our CD studies, and now an ongoing NMR investigation of the LaC2 solution structure,[47] suggest that the apoprotein has significant helical structure, but coordinating the metal alters the tertiary protein structure near the metal site, and perhaps even globally.

Interestingly, the difference between the peptide LnP3W and the metallohomeodomain LnC2 in reactivity was striking. We found that a stable, well-folded domain may not be ideally organized for cleavage, perhaps because of differences in the accessibility of the metal center to either DNA or smaller model phosphate substrates. The solution structure of LaC2 will prove to be critical in addressing these questions.

With any challenge comes opportunities, and the successful design of a folded metallohomeodomain now allows us to begin to reintroduce changes in the active site and systematically manipulate substrate accessibility in these domains, as we have done with the series of smaller peptide chimeras. Furthermore, in the simplest sense, we have demonstrated that substituting β turns with metal-binding turns does not necessarily require homologous parental scaffolds but rather relies on the structural similarity of the motifs flanking the turn. Thus, any ligand-rich sequence capable of spanning a 90° corner between helices could potentially be built into a HTH scaffold. As mentioned earlier, a number of metal sites match these criteria, which opens the door to creating new reactivity within a DNA-binding scaffold. There is, therefore, still much room for the powerful tool of protein design to enrich our understanding of metal function in biology and to explore the reactivity of bioinorganic active sites.

Materials and Methods

Peptide Synthesis. The chimeric peptides were prepared in house by manual solid-phase peptide synthesis using orthogonal protection consisting of N-terminal fluorenylmethoxycarbonyl (Fmoc) protecting groups and various side-chain protecting groups where necessary. The solid support resin used was PAL−PEG−PS. Fmoc deprotection was accomplished with a solution of 20% piperidine in dimethylformamide (DMF), and coupling was achieved with 1-hydroxybenzotriazole and 1,3-diisopropylcarbodiimide. The coupling and deprotection were confirmed by testing samples with a solution of DMF, diisopropylethylamine, and picrylsulfonic acid. The peptides were cleaved from the resin with a solution of trifluoroacetic acid, triisopropylsilane, and water (95:2.5:2.5). The peptides were precipitated with ether, redissolved in water, and then lyophilized to a fluffy white solid. The peptides were purified to ≥95% purity by reversed-phase HPLC on a Hamilton PRP-3 semipreparative column using a linear gradient of 10−90% acetonitrile in water and 0.1% trifluoroacetic acid on an Agilent 1100 series high-performance liquid chromatograph. The correct mass was validated by electrospray ionization mass spectrometry using a ThermoFinnigan LCQ mass spectrometer (University of Iowa Mass Spectrometry Facility, NIH grant 510 RR13799-01).

Protein Cloning and Expression. The preparation of the C2 clone and further expression details will be published elsewhere[45] but briefly is as follows. Cells containing the gene-encoding C2 (designed by selective deletion and insertion of the turn region of an *engrailed* homeodomain) were grown at 37 °C, lysed with lysosome, and treated with DNaseI in appropriate buffers. Because the target protein was found in the cell lysate pellet, the pellet was collected after centrifugation. The cell pellet was passed through a French press and centrifuged, and soluble protein precipitated from the supernatant with 30% $(NH_4)_2SO_4$. The protein was resolubilized in a mildly denaturing extraction buffer (20 mM Tris-HCl (pH 8.0), 1 M urea, 1% Triton X-100, 1 M NaCl) and then dialyzed overnight to reduce NaCl to 75 mM. Proteins were further purified by DEAE Sepharose 6B (Sigma), Heparin Sepharose 6FF (Amersham), and Shephadex G-50 columns. Protein was made metal-free using dialysis and a desalting column (Sephadex G-25).

Tb Fluorescence Titrations. Fluorescence emission spectra were recorded on a ThermoSpectronic Aminco-Bowman series 2 luminescence spectrometer in a 1-cm-path-length quartz cuvette. Solutions of 30 μM peptide or 10 μM C2 protein in a 10 mM HEPES buffer (pH 6.9) were prepared and titrated to 10 equiv of metal

with $TbCl_3$ stock containing peptide (or protein) at the appropriate concentration to maintain a constant peptide (or protein) concentration during the titration. The samples were incubated for 5 min after each metal addition before recording the emission spectra. Samples were excited at 290 nm, and the emission was monitored from 450 to 650 nm ($\lambda_{max} \sim 545$ nm). For each measurement, three scans were collected at a scan rate of 6 nm/s and averaged together. A 495-nm long-pass filter was used to avoid interference from Rayleigh scattering. The data from each titration were fit to the following equation as described in ref 25, which assumes 1:1 binding between the metal and peptide when possible.

$$\Delta S = \Delta S_{max} \frac{([P]_T + [M]_T + K_d) - \sqrt{([P]_T + [M]_T + K_d)^2 - 4[P]_T[M]_T}}{2[P]_T} + C[M]_T$$

ΔS and ΔS_{max} are the signal change and total signal change from specific binding, and C is the contribution from nonspecific binding. In the case of TbP3W, the last term ($C[M]_T$) was omitted because of the lack of any nonspecific character in the data.

CD Studies. The solution structure of each peptide was examined by CD alone and in the presence of increasing concentrations of $EuCl_3$ on an Olis DSM-17 Conversion Spectrometer. Solutions of 30−60 μM peptide with a 20 mM Tris buffer (pH 7.2) were prepared and then titrated with $EuCl_3$ (1 mM stock). A scan was taken after each addition of metal over the range of 180−280 nm (2-nm intervals with a fixed integration time of 1.7 s). Spectra were baseline-corrected to 0 mdeg at 280 nm. Titration curves [P3W(D) and P3N] were created by plotting the $EuCl_3$ concentration versus CD signal at 222 nm (Figures S4 and S5 in the Supporting Information; Figure 4 presents apo and 1:1 Eu−peptide spectra). For P3E and P3A, little change in ellipticity was observed upon the addition of metal. For metalloprotein C2 (Figure 5), the apo and Tb^{III}C2 spectra were recorded as above (10 mM HEPES buffer (pH 6.9); 10 mM $TbCl_3$ stock; 1 s/nm).

Acknowledgment. This work has been supported by the National Science Foundation [Grants CHE-0093000 (CAREER) and MCD-0451199]. We thank Ms. Siu Wah Wong-Deyrup for assistance in preparing the C2 clone.

Supporting Information Available: Tb-FRET titrations of peptides P3A, P3E, and P3N as a function of the Tb(III) concentration and CD folding titration studies of P3W(D) and P3N as a function of Eu(III). This material is available free of charge via the Internet at http://pubs.acs.org.

IC060877K